Journal of Alloys and Compounds 509 (2011) 2784–2788

Contents lists available at ScienceDirect

Journal of Alloys and Compounds

journal homepage: www.elsevier.com/locate/jallcom

Effect of catalyst calcination temperature on the synthesis of MWCNT–alumina hybrid compound using methane decomposition method

Muhammad Helmi Abdul Kudus, Hazizan Md. Akil*, Hasmaliza Mohamad, Lim Eng Loon

School of Materials and Mineral Resources Engineering, Engineering Campus, Universiti Sains Malaysia, 14300 Nibong Tebal, Pulau Pinang, Malaysia

ARTICLE INFO

Article history:
Received 12 July 2010
Received in revised form
12 November 2010
Accepted 15 November 2010
Available online 13 December 2010

Keywords:
MWCNT–alumina
Hybrid compound
Catalyst
Calcination temperature

ABSTRACT

This work focuses on synthesis of MWCNT–alumina hybrid compound via methane decomposition process using Ni–Al_2O_3 catalyst. The catalysts prepared through in situ process by using nickel salt and aluminium powder which are then calcined at three different calcination temperatures (700 °C, 900 °C and 1100 °C). The catalyst calcined at 900 °C followed by methane decomposition process successfully yielded MWCNT–alumina hybrid compound. No trace of CNT was detected for catalyst calcined at 700 °C and 1100 °C. The scanning electron microscopy (SEM) and high resolution transmission electron microscopy (HRTEM) micrograph confirmed the formation of MWCNT with homogenous dispersion on alumina particles.

© 2010 Elsevier B.V. All rights reserved.

1. Introduction

Hybrid compound is becoming more popular than single compound in order to obtain a new set of material properties [1–5]. Although combination of materials can be done in many ways such as direct blending, mechanical milling, sonication mixing and sol–gel method, chemical synthesis remains the best technique among all. Chemical syntheses have been widely used to produce various hybrid compounds including carbon nanotubes-based hybrid compound. Carbon nanotubes (CNT) are considered to be one of the most excellent nano-scale materials due to its remarkable chemical and physical properties. As a result, CNT has been used in various applications either on its own or as reinforcement in composite material. Various synthesis methods have been developed for the production of CNT in the past [6–13]. Methane decomposition is one type of chemical vapour deposition (CVD) process which is an efficient method to produce CNT. In CVD process, many factors affect the growth of CNT such as catalyst preparations, calcination temperature, calcination duration, reduction time, reaction time, feedstock gas and gas flow rate. CNT on its own possesses several processing problems especially when uniform mixing is required in preparing composite material [8]. Studies had shown that CNT can be combined with other materials such as silica [14,15], chitosan [16–19], iron oxide [20,21], aluminasilicate [22], titania [23], as well as alumina [7,8,24]. However, alumina is known to have high temperature resistance, and possesses high hardness. Combining CNT and alumina powder by simply blending them together give inefficient combination, where some of the CNT will not bond to alumina. These unbounded CNT tends to agglomerate together during polymer composite preparation, thus, leading to the obstruction of efficient load transfer to the polymer matrix [12]. To synthesis CNT via CVD, catalyst selection is one of crucial part. Many types of catalysts have been produced that vary in their metal support and the most common catalysts are nickel, cobalt, iron, or a combination [7–32]. Among these metal, nickel is always used as metal catalyst for CNT growth. Nickel is chosen because it is used extensively as a catalyst in industrial process as steam reforming, methanation, hydrogenation and dehydrogenation reactions [7]. There are many types of nickel salts that can be used in NiO catalyst production such as $Ni(NO_3)_2{\cdot}6H_2O$, $NiCl_2{\cdot}6H_2O$, $NiSO_4{\cdot}6H_2O$ and $Ni(HCOO)_2{\cdot}6H_2O$ [10,27,33]. Nickel nitrate hexahydrate salts, $Ni(NO_3)_2{\cdot}6H_2O$, is always chosen [7,8,10,27,28,31,33] because it gives significant effect on the particles size of NiO (Table 1). Chen et al. [10] reported that nickel nitrate is good for preparation of NiO/Al_2O_3 in order to meet high dispersion and great surface area of supported nickel oxide. In this work, Ni–alumina catalyst prepared via in situ–precipitation, calcination and reduction process which was then underwent methane decomposition to grow multiwalled CNT (MWCNT). Effect of the catalyst calcination temperature which correlated to the yield of MWCNT growth also investigated and the possible explanations on the effect are discussed.

---

* Corresponding author. Tel.: +60 40 5996161, fax: +60 04 5941011.
E-mail address: hazizan@eng.usm.my (H.Md. Akil).

0925-8388/$ – see front matter © 2010 Elsevier B.V. All rights reserved.
doi:10.1016/j.jallcom.2010.11.099

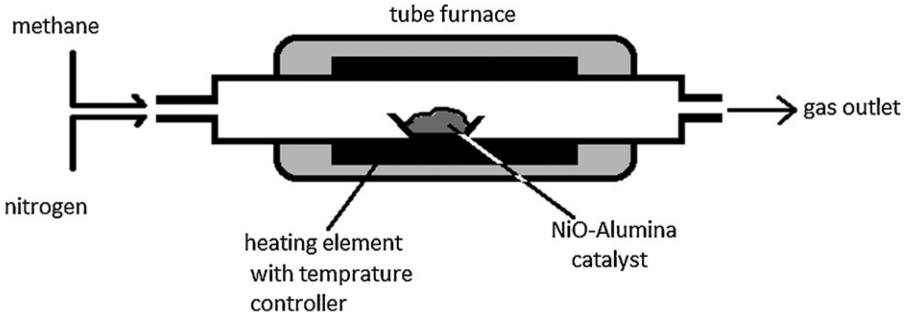

Fig. 1. Schematic equipment set up for CNT growth to from CNT–alumina hybrid.

Table 1
Effect of nickel salt on particle size of NiO over alumina.

Nickel salts	Particle size of NiO, (Å)
$Ni(NO_3)_2{\cdot}6H_2O$	40
$NiCl_2{\cdot}6H_2O$	78
$NiCl_4{\cdot}6H_2O$	–
$Ni(HCOO)_2{\cdot}6H_2O$	127

2. Experimental

2.1. Catalyst preparation

The catalyst was prepared by mixing aluminium powder (0.38 mol, 99% purity) with $Ni(NO_3)_2{\cdot}6H_2O$ (0.01 mol, 98% purity) in 1 l of distilled water. NaOH (0.02 mol 98% purity) was dissolved in distilled water (50 ml) and added into previous mixture with constant stirring. The colloid formed and then aged at room temperature for 24 h without stirring. After 24 h the green paste was washed and filtered and followed by drying at 110 °C for 2 h. Consequently, the catalyst was calcined at 700 °C, 900 °C and 1100 °C, respectively. Finally the reduction of catalyst was done under hydrogen gas 400 °C for 2 h.

2.2. Growth of MWCNTs

The MWCNT growth on alumina was conducted in custom-made CVD setup horizontal tube furnace with precise gas flow control unit. The reduced catalyst then reacted in CH_4/N_2 mixture at 800 °C for 30 min to grow MWCNT in the tube furnace with a significant flow rates ratio of CH_4 to N_2 of 1:7. Fig. 1 shows a schematic diagram of customize horizontal furnace used in this study.

2.3. Characterizations of MWCNT–alumina compound

The yields were analysed using X-Ray Diffraction (XRD) method. Intensity was measured by step scanning in the 2θ range of 10°–80°. The morphology of MWCNT–alumina was analysed using Leo Supra-35VP field emission scanning electron microscope (FESEM) and high resolution transmission electron microscope (HRTEM-Model Philip TECNAI 20 (200 kV)). The compositions of carbon (C) and alumina (Al_2O_3) were analysed using energy dispersive X-ray spectroscopy (EDX).

3. Results and discussion

3.1. The effect of catalyst calcination temperature on the yield of MWCNTs–alumina

Based on various calcination temperatures, the yield of MWCNT–alumina compound was quantitatively measured. MWCNT–alumina was successfully produced through catalyst that calcined at 900 °C after underwent catalytic methane decomposition. By using EDX, the weight percentage of carbon and alumina were determined as a function of catalyst calcination temperature (700 °C, 900 °C and 1100 °C) which is presented in Fig. 2. The highest carbon content, 12.81% was obtained from catalyst calcined at 900 °C. This temperature believed to be an optimum calcination temperature to perform the catalytic decomposition by reacting in methane at 800 °C. The catalyst that calcined at 700 °C and 1100 °C was inactive in methane decomposition and very small amount of deposited carbon was observed on the catalyst surfaces.

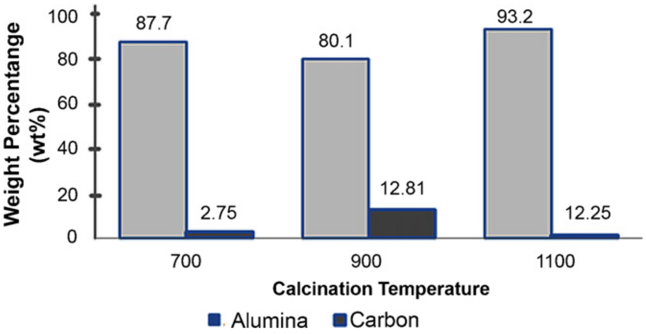

Fig. 2. Effect of catalyst calcination temperature on the formation of carbon (wt.%) obtained from EDX analysis.

3.2. Characterization of MWCNT–alumina hybrid

Fig. 3a and b show typical HRTEM images of MWCNT obtained after 30 min reaction in methane by using catalyst calcined at 900 °C. The MWCNT appear to be rope-like structures with outer diameters ranging from 10 to 30 nm and inner diameters in the range of 4–8 nm and attached to the micro-sized alumina particle. From the HRTEM micrograph, the nickel particles found to be either capped on one nanotube end or being encapsulated by carbon-tube. One can notice that the outer diameter of grown MWCNTs is about the same as nickel particle size as shown in Fig. 3c. The CNT is confirmed as MWCNT by the existence of hollow structure and multi-layered wall which is demonstrated in Fig. 3d. The MWCNT morphology contains several layers of graphene sheets along the longitudinal direction of nanotube. The produced MWCNT having about ~10–40 graphene layers which formed the basis of catalytic activity of nickel particles. The variation of graphene layers formed could be attributed to the morphology of synthesized nickel particles. The synthesized nickel particles had irregular shapes before synthesizing MWCNTs, but the particles that plunged at the end of the MWCNT tips had consistent shape. The unreacted nickel particles sizes existed on alumina surface had smaller size than nickel particle at the end tips of CNT which is shown in Fig. 3a. This observation seems to be parallel to Li et al. [34].

Fig. 4a and c show that the morphology of catalyst calcined at 700 °C and 1100 °C after performing methane decomposition. The morphologies of both samples were about the same which show

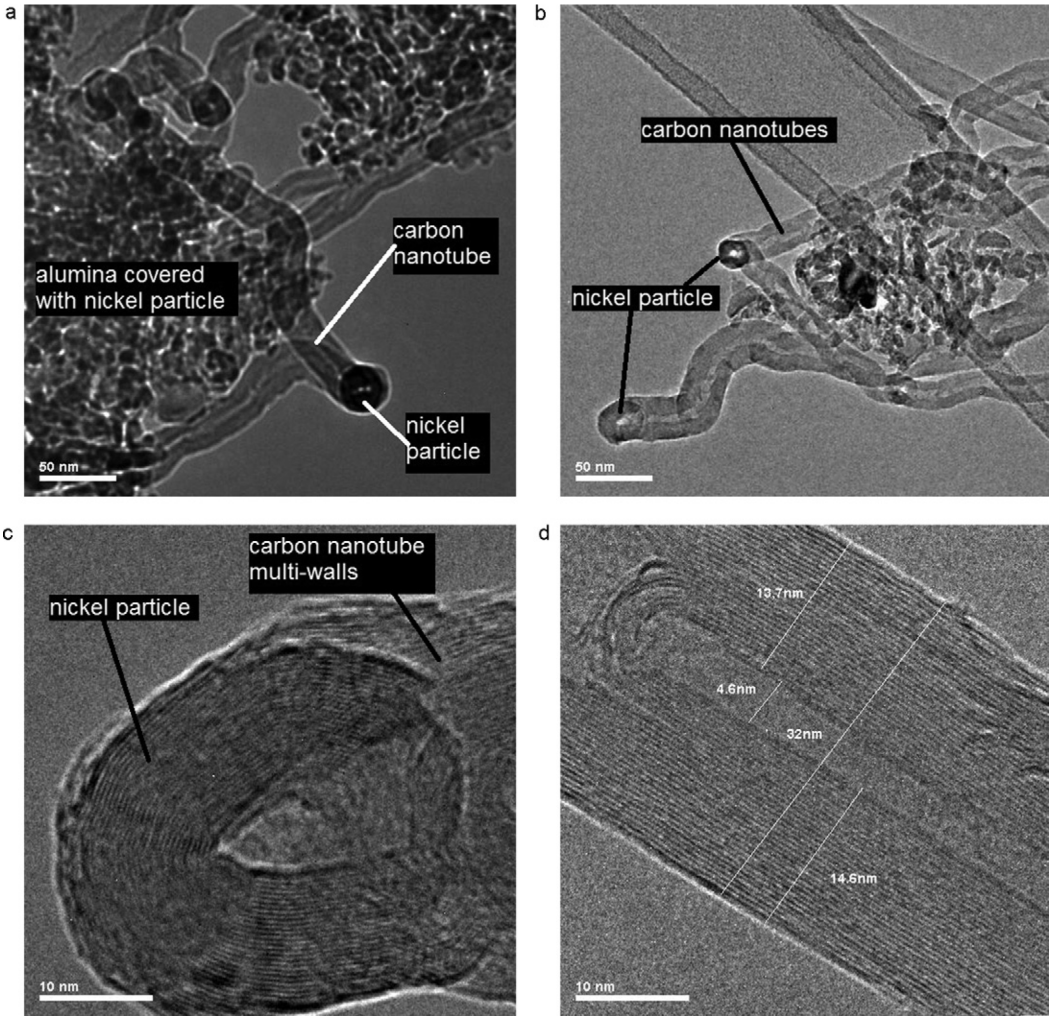

Fig. 3. HRTEM images of CNTs grown on catalyst calcined at 900 °C in CNT–alumina hybrid synthesize.

the wrinkled particles which were believed to be nickel particles scattered on rod-like alumina particles. No MWCNT detected in both SEM images. The same morphology of samples which calcined at 700 °C and 1100 °C had also been proved by Kiss et al. [33].

Figs. 4b and 5 show the distribution of MWCNT on alumina surface. This homogenous distribution of MWCNT on alumina surface is necessary to optimize the effect of MWCNT–alumina hybrid properties as reinforcement in polymer matrix composites. The ability of alumina to disperse homogenously in polymer matrix serves as vehicle for MWCNT. With the presence of alumina, it is expected that MWCNT can be dispersed more homogenously in polymer matrix even by using conventional processing method [8], where the homogeneity is the main obstacle when using MWCNT as a single reinforcement for polymer composites.

The different catalyst calcination temperature is expected to give different chemical composition of CNT/alumina which can be confirmed by X-ray diffraction pattern. Summary XRD pattern of alumina/CNT synthesized using Ni catalyst calcined at 700 °C, 900 °C and 1100 °C is given in Fig. 6a–c. From Fig 6a and b, the formation carbon, C (ICDD 01-075-1621), alumina (ICDD 01-074-2206) and NiO (ICDD 01-078-0429) is confirmed. The colour change of the catalyst from light blue to black also proved the presence of carbon in the sample.

On the other hand, there is no obvious peak to confirm the presence of carbon in Fig. 6a and c. This shows that there is no MWCNT growth on catalyst calcined at 700 °C and 1100 °C respectively which also confirmed by SEM images and very low amount of carbon found in EDX analysis. For both XRD patterns, only Al_2O_3 and Ni phase detected via XRD. The peaks corresponding to spinel $NiAl_2O_4$ (ICDD 03-065-3102) were also detected in XRD pattern of catalyst that calcined at 1100 °C after reacted in methane decomposition (Fig. 6c).

In summary, the catalyst calcined at 900 °C provides the most suitable $NiO–Al_2O_3$ interaction for the further reaction during methane decomposition. During reaction in methane gas, the size of nickel catalyst particles remain unchanged and suitable interaction provide higher catalytic activities to grow MWCNT [9]. The reaction of carbon forming by the catalytic decomposition of methane is as follows:

$$CH_4 \rightarrow 2H_2 + C$$

Chai et al. [9] reported that at lower calcination temperature, the carbon yield is lower. Increasing the calcination temperature will increase the carbon yield. It is believed that the lower carbon yield is due to weak interaction between nickel oxide and alumina when calcined at lower temperature (700 °C) which provides less

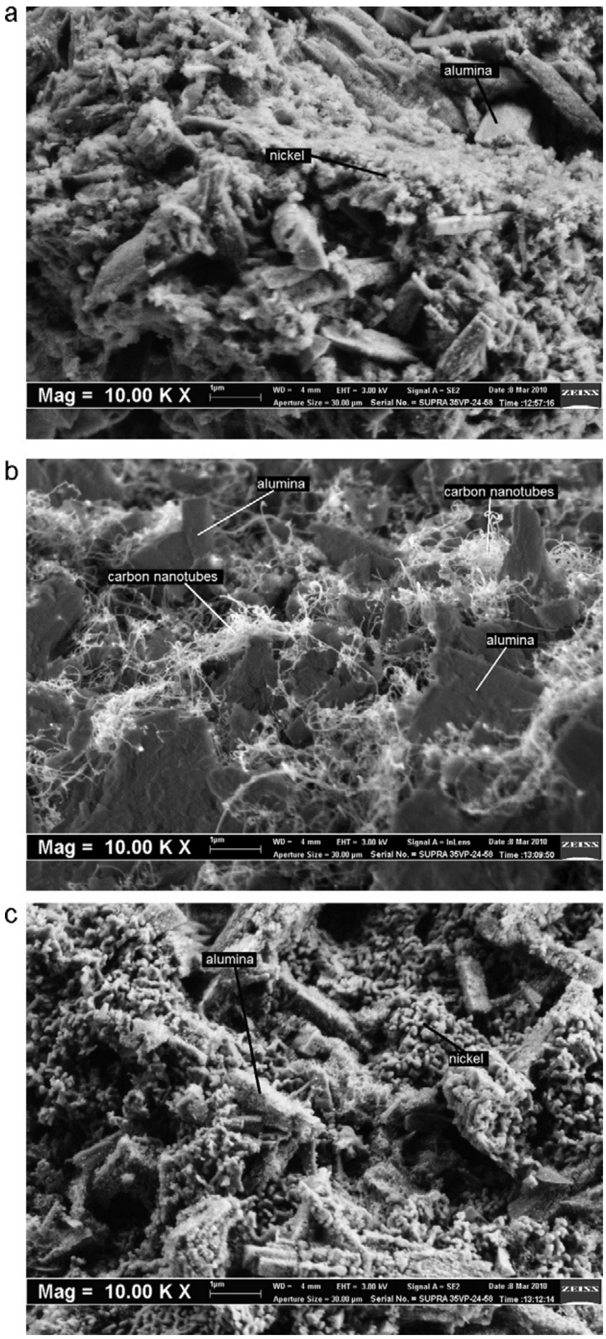

Fig. 4. SEM micrograph of CNT–alumina hybrid synthesized using catalyst calcined at (a) 700 °C, (b) 900 °C at 10KX, and (c) 1100 °C.

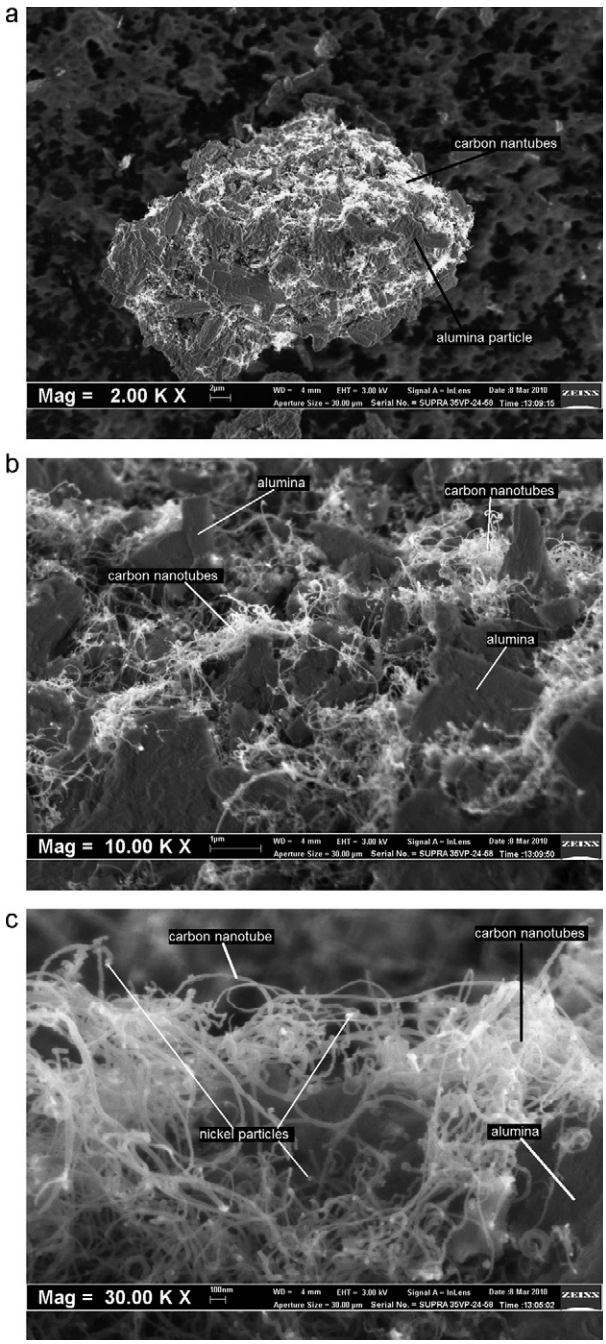

Fig. 5. SEM micrographs of CNT distribution on alumina in CNT–alumina hybrid system with magnification of (a) 2000×, (b) 10,000× and (c) 30,000×.

catalytic activities to grow MWCNT. The increase in reaction temperature from 700 °C to 800 °C could be attributed to the increase in crystallites size of nickel oxide [10]. In other words, the increase in reaction temperature caused nickel oxide to be sintered from smaller crystallites to form larger crystallites of various sizes. The increase in crystallites size will result in the formation of larger nickel oxide clusters which eventually unable to grow MWCNTs on alumina [9]. In this study, it was found that among the three calcination temperatures, the catalyst calcined at 900 °C provides the most suitable NiO–Al_2O_3 interaction at the reaction temperature of 800 °C. This is because no larger cluster of catalyst formed and suitable interaction provide higher catalytic activities to grow MWCNTs. However, at high calcination temperature (1100 °C), the carbon yield is the lowest among the three catalyst calcination temperatures. It is believed that at high temperature, nickel oxide reacted strongly with alumina to form nickel aluminate spinel ($NiAl_2O_4$) which reduced the catalytic activities in methane decomposition. The formation of $NiAl_2O_4$ spinel was confirmed by the XRD analysis. The formation of $NiAl_2O_4$ spinel is due to the diffusion of nickel species into the alumina lattice which may hinder the accessibility of the active nickel species to the reactant. The formation of spinel compound $NiAl_2O_4$ at high-calcination temperature also reported earlier by Kiss et al. [33], Chen et al. [10] and Joo and Jung [26].

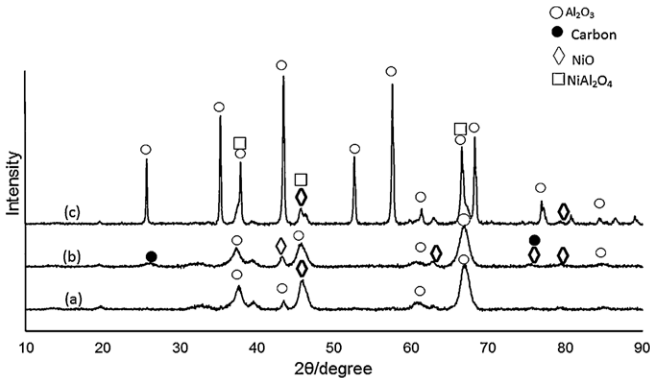

Fig. 6. XRD Pattern of CNT–alumina produced using catalyst calcined at (a) 700 °C, (b) 900 °C and (c) 1100 °C.

4. Conclusion

From the analysis, the calcination at temperatures range from 700 °C to 1100 °C gives different percentage of MWCNT yield. The catalyst calcination temperature of 900 °C is an optimum temperature for catalytic activities of the Ni–alumina catalyst during methane decomposition process. The SEM micrographs showed the entangled nanosize carbons on the alumina surface which proof the high catalytic activities of the catalyst in methane conversion to form nanosizes carbon tubes (MWCNT). This method shows that the CNTs were homogenously distributed on alumina surface to optimize the performance of CNT–alumina hybrid system.

Acknowledgement

The authors would like to gratefully acknowledge Universiti Sains Malaysia for all the assistance that has resulted in this article.

References

[1] V.K. Rangari, G.M. Mohammad, S. Jeelani, A. Hundley, K. Vig, S.R. Singh, S. Pillai, Nanotechnology 21 (2010) 09510.
[2] N. Bruque, R.R. Pandey, R.K. Lake, H. Wang, J.P. Lewis, Molecular Simulation 31 (12) (October 2005) 859–864.
[3] J. Zhai, Y. Zhai, D. Wen, S. Dong, Electroanalysis 21 (20) (2009) 2207–2212.
[4] S.G. Chou, H.B. Ribeiro, E.B. Barros, A.P. Santos, D. Nezich, G.G. Samsonidze, C. Fantini, M.A. Pimenta, A. Jorio, F. Plentz Filho, M.S. Dresselhaus, G. Dresselhaus, R. Saito, M. Zhengi, G.B. Onoa, E.D. Semke, A.K. Swan, M.S. Ünlü, B.B. Goldberg, Chemical Physics Letters 397 (2004) 296–301.
[5] M. Jacob, S. Thomas, K.T. Varughese, Journal of Applied Polymer Science 93 (5) (2004) 2305–2312.
[6] S. Porro, S. Musso, M. Vinante, L. Vanzetti, M. Anderle, F. Trotta, A. Tagliaferro, Phsyca E 37 (2007) 58–61.
[7] C.N. He, F. Tian, S.J. Liu, Journal of Alloys and Compounds 478 (2009) 816–819.
[8] C.N. He, F. Tian, Scripta Materialia 61 (2009) 285–288.
[9] S.-P. Chai, S.H.S. Zein, A.R. Mohamed, Carbon 45 (2007) 1535–1541.
[10] I. Chen, S.-Y. Lin, D.W. Shiu, Industrial and Engineering Chemistry Research 27 (6) (1988) 926–929.
[11] I. Chen, D.W. Shiu, Industrial and Engineering Chemistry Research 27 (3) (1988) 429–434.
[12] J.Y. Kim, D.K. Kim, S.H. Kim, European Polymer Journal 45 (2009) 316–324.
[13] C.N. He, N.Q. Zhao, C.S. Shi, S.Z. Song, Journal of Alloys and Compounds 484 (2009) 6–11.
[14] R. Sivakumar, S. Guo, T. Nishimura, Y. Kagawa, Scripta Materialia 56 (2007) 265–268.
[15] J. Umeda, K. Kondoh, H. Imai, Materials Science and Engineering A 504 (2009) 157–162.
[16] I. Olivas-Armendáriz, P. García-Casillas, R. Martínez-Sánchez, A. Martínez-Villafañe, C.A. Martínez-Pérez, Journal of Alloys and Compounds 495 (2010) 592–595.
[17] L. Carson, C. Kelly-Brown, M. Stewart, A. Oki, G. Regisford, Z. Luo, V.I. Bakhmutov, Materials Letters 63 (2009) 617–620.
[18] S.-H. Baek, B. Kim, K.-D. Suh, Colloids and Surfaces A: Physicochemical and Engineering Aspects 316 (2008) 292–296.
[19] G.M. Spinks, S.R. Shin, G.G. Wallace, P.G. Whitten, S.I. Kim, S.J. Kim, Sensors and Actuators B 115 (2006) 678–684.
[20] X. Wang, Z. Zhao, J. Qu, Z. Wang, J. Qiu, Journal of Physics and Chemistry of Solids 71 (2010) 673–676.
[21] B.T. Hang, H. Hayashi, S.-H. Yoon, S. Okada, J.-I. Yamaki, Journal of Power Sources 178 (2008) 393–401.
[22] K.J. Lee, Y.T. Yeh, H.Z. Cheng, P.C. Chang, S.W. Lin, Y.D. Chen, Journal of Alloys and Compounds 504S (2010) S356–S360.
[23] M.-L. Chen, F.-J. Zhang, W.-C. Oh, New Carbon Materials 24 (2) (2009) 159–166.
[24] D.-S. Lim, D.-H. You, H.-J. Choi, S.-H. Lim, H. Jang, Wear 259 (2005) 539–544.
[25] H. Li, N. Zhao, C. He, C. Shi, X. Du, J. Li, Journal of Alloys and Compounds 468 (2009) 64–68.
[26] O.-S. Joo, K.-D. Jung, Bulletin of Korean Chemical Society 23 (8) (2002).
[27] I.W. Lenggoro, Y. Itoh, N. Iida, K. Okuyama, Materials Research Bulletin 38 (2003) 1819–1827.
[28] J. Juan-Juan, M.C. Román-Martínez, M.J. Illán-Gómez, Applied Catalysis A: General 264 (2004) 169–174.
[29] N. Inami, M.A. Mohamed, E. Shikoh, A. Fujiwara, Science and Technology of Advanced Materials 8 (2007) 292–295.
[30] L. Jodin, A.-C. Dupuis, E. Rouvière, P. Reiss, Journal of Physical Chemistry B 110 (2006) 7328–7333.
[31] N.Q. Zhao, C.N. He, J. Ding, T.C. Zou, Z.J. Qiao, C.S. Shi, X.W. Du, J.J. Li, Y.D. Li, Journal of Alloys and Compounds 428 (2007) 79–83.
[32] J.-.W. An, D.-H. You, D.-S. Lim, Wear 255 (2003) 677–681.
[33] E. Kiss, G. Bošković, M. Lazić, G. Lomić, R. Marinković-Nedučin, Scanning 28 (2006) 236–241.
[34] Z. Li, J. Chen, X. Zhang, Y. Li, K.K. Fung, Carbon 40 (2002) 409–415.